Radar cross-section of a wind turbine: application to weather radars

Thomas Lepetit, Jérôme Simon, Jean-François Petex, Anil Cheraly, Jean-Paul Marcellin

Radar cross-section of a wind turbine: application to weather radars

T. Lepetit[1], J. Simon[1], J.-F. Petex[1], A. Cheraly[1], J.-P. Marcellin[1]
[1] DEMR, ONERA, Université Paris Saclay, F-91123 Palaiseau – France
thomas.lepetit@onera.fr

***Abstract*—We report RCS measurements of wind turbines in the C-band for both HH and VV polarizations. These show a common scattering mechanism between the two polarizations albeit with a large difference in amplitude. These results have a strong implication for polarimetric metrics used in weather radar algorithms. We thus highlight the need for dual-polarization radars or fine-grained simulations to properly assess the impact of wind turbines on weather forecast.**

***Index Terms*—wind turbines, radar cross-section, shooting-bouncing ray.**

I. INTRODUCTION

In the last two decades, the proportion of renewable sources of energy, *e.g.* geothermal, hydropower, solar and wind, has steadily risen worldwide. This trend is bound to continue due to the necessity of replacing fossils fuels to minimize the impact of global warming. As of early 2018, more than 500 GW of wind power capacity was installed all around the planet [1]. In Denmark, wind power (on-shore and off-shore) accounted for as much as 43.6% of electricity consumption in 2017 [2].

However, renewables all have an impact. For instance, wind turbines have been known to increase bird, insect, and bat fatalities [3]. Another major concern is the impact of wind farms, *i.e.*, collections of wind turbines, on surrounding radars. Indeed, nowadays, both civilian and military radars ensure critical missions; weather radars must alert ahead of time of dangerous thunderstorms, air traffic control radars must avoid collision between an ever increasing amount of airplanes, and surveillance radars must locate non-authorized aircrafts around sensitive areas. In the last fifteen years, multiple countries and authorities have launched programs to evaluate and mitigate wind farms perturbations [4].

In short, wind turbines affect radars mainly for three reasons. First, these are very large and visible structures, upward of 240 m for the tallest [5]. Second, towers are made of highly reflecting materials, originally steel and, more recently, concrete [6]. Finally, blades tip reach a large velocity, upward of 100 m/s for the longest [7]. All three reasons combine to make for a large radar cross-section (RCS), both static and dynamic, and pose trouble to clutter cancelation algorithms. Besides, the current trend is toward taller hubs and larger rotors, which will only amplify the impact of wind turbines in years to come.

In this paper, we focus solely on the case of interference between wind farms and C-band weather radars. We first present co-polarized RCS measurements with our own mobile radar, in both horizontal (HH) and vertical (VV) polarizations, and then discuss the proper balance between accuracy and execution time for simulation tools.

II. MEASUREMENTS

A. Mobile radar

All measurements were carried out with our own mobile radar (MEDYCIS) in C-band. In this frequency range, we have a 400 MHz bandwidth (5.45-5.85 GHz), *i.e.*, centered on that of Météo-France (5.60-5.65 GHz), the French public entity responsible for all weather forecast [8]. Besides, we have a 4° half-power beamwidth, for both polarizations (HH-VV), consistent with a waveguide-fed parabolic reflector, and a maximum range of 20 km. Finally, our antenna stands at the top of a 6.5 m mast and, thus, we mostly avoid low-elevation clutter.

The measurement campaign was carried out in the north of France, around Abbeville. We were allowed by Arcep, the French authority in charge of electronic communications [9], to emit from 5.70 to 5.80 GHz (1.5 m resolution).

Figure 1: Mobile radar with antenna on top of its mast, followed by emission/reception units, living quarters, and power source (left). Three measured wind turbines as seen from up close (right)

Figure 1 shows the mobile radar along with a close-up view of some of the measured wind turbines. The furthest wind turbine was no more than 5.2 km away and, thus, we were able to use an optical camera, aligned with the radar axis, to make sure that we pointed right at the nacelle.

B. Spectrograms

We collected several frequency responses for a duration long enough to ensure at least one complete rotation of wind turbine blades. Our Pulse Repetition Frequency (PRF) was chosen to satisfy both our Doppler (±3.3 kHz) and range (±250 m) requirements. Our range measurement was tightly

centered on wind turbines to avoid unnecessary surface clutter.

To remove all static contributions, to mimic radar signal processing algorithms, we high-pass filtered all of our measurements.

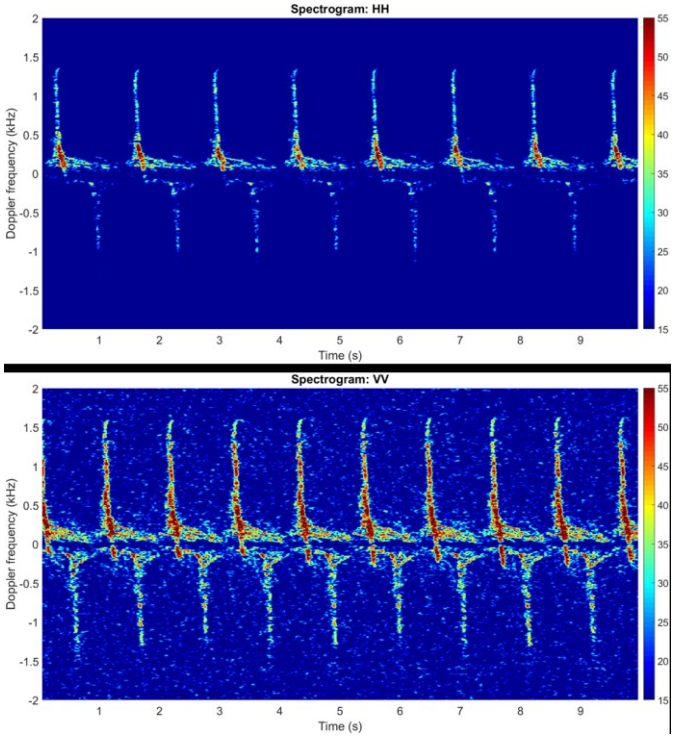

Figure 2: Spectrograms of one wind turbine measured at 5.7 GHz during a 10 s stretch (in dBm²). HH (top) and VV (bottom) polarizations. All measurements were high-pass filtered to remove static contributions.

Figure 2 shows the spectrograms of one wind turbine measured for both HH and VV polarizations. Spectrograms looks the same, *i.e.*, most scattering mechanisms are shared by both polarizations. We do observe alternating flashes at positive/negative Doppler frequencies, due to leading/trailing edges of wind turbine blades. The main difference lies in the amplitude of these contributions, which are much greater for VV polarization.

C. *Radar reflectivity factor*

In meteorology, a quantity called Radar Reflectivity Factor (RRF), written Z, is used to quantify the radar return of distributed targets such as hydrometeors (raindrops, hail, snow, etc.). It can be derived from RCS and radar properties by the Probert-Jones equation [10]:

$$Z_{dBZ} = \sigma_{dBm^2} + 40log(\lambda_m) - 10log(V_{m^3}) + 155 \quad (1)$$

Equation 1 relates RFF to RCS, wavelength, and probed volume (distance, pulse and beam widths).

Note that the constant term is related to the nature of the considered hydrometeor, in our case wind turbines, and we use Equation 1 to convert from dBm^2 to dBZ for both polarizations (Z_{HH}, Z_{VV}).

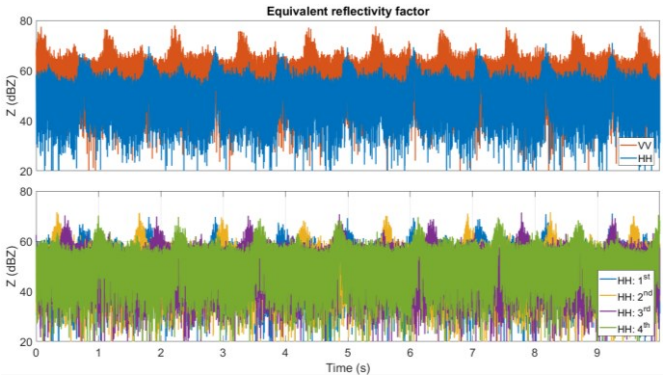

Figure 3: Radar reflectivity factors of one wind turbine measured during a 10 s stretch (in dBZ). Comparison of HH and VV polarizations for the 1st measurement (top). Comparison of four measurements for HH polarization (bottom).

Figure 3 shows a comparison of RRF for HH and VV polarizations on a given wind turbine. Just as for RCS, there is a large difference in favor of VV polarization. Since these two polarizations were not simultaneously measured, the difference could be due to the relative orientation of the wind turbine and the radar. However, as shown by the four HH polarization measurements that were all carried out at different times, hence in different wind configurations, this difference cannot be solely explained by this hypothesis. RFF is thus a polarization-dependent quantity.

European and American weather forecast agencies rely on a common set of metrics, beyond Z_{HH} and Z_{VV}, to classify hydrometeors. This classification relies on fuzzy logic as applied to polarimetric information such as differential reflectivity, co-polarized cross-correlation coefficient (modulus and phase) [11]:

$$Z_{DR} = Z_{HH} - Z_{VV} \quad (2)$$

$$\rho_{HV} \propto \left| \frac{\sqrt{\sigma}^*_{HH}\sqrt{\sigma}_{VV}}{\sqrt{|\sqrt{\sigma}_{HH}|^2 |\sqrt{\sigma}_{VV}|^2}} \right| \quad (3)$$

$$\varphi_{HV} \propto arg\left[\frac{\sqrt{\sigma}^*_{HH}\sqrt{\sigma}_{VV}}{\sqrt{|\sqrt{\sigma}_{HH}|^2 |\sqrt{\sigma}_{VV}|^2}} \right] \quad (4)$$

Where $\sqrt{\sigma}_{ij}$ is a component of the complex RCS [12]. Therefore, it is mandatory to measure simultaneously HH and VV polarizations to compute these quantities. Unfortunately, our radar is not yet dual-polarization and, therefore, we do not have such measurements.

In the following, we turn to simulations to consider the classification of wind turbines by weather radar algorithms.

III. SIMULATIONS

A. *Asymptotic methods*

The vast majority of wind turbine RCS computations presented thus far were carried out with asymptotic methods

[13], such as Geometrical Optics (GO), Physical Optics (PO) or a mix of both commonly known as Shooting Bouncing Ray (SBR) [14]. This is due to the very large electrical size of wind turbines (>1500λ). For full-wave methods that require a fine mesh, usually below λ/5, this represents tens of thousands wavelengths and is often not compatible with intensive computations requirements.

However, SBR codes are inherently approximate and thus do not include all polarization-dependent scattering mechanisms. Most do include edge diffraction, *via* the Equivalent Current Method (ECM, [15]) or the Incremental Length Diffraction Coefficient (ILDC, [16]), but few can account for creeping waves [17]. On top of that, not all parts of a wind turbine are impenetrable, *e.g.* nacelle and blades are often made of glass-fiber composites, and transmission through these needs to be modeled. Newer generation wind turbines also have carbon-fiber parts within blades, for stiffer reinforcement, which have a large RCS that cannot be ignored [18]. Therefore, an accurate simulation of the differences in RCS between HH and VV polarizations is a tall order for purely asymptotic methods.

In recent years, hybrid methods combining asymptotic and full-wave methods, have been developed. Most notably Method of Moments (MoM) and SBR have been hybridized for antenna gain diagram computation [19]. Still, at present, wind turbines seem to be out of reach even for these hybrid methods due to a combination of electrical size, dielectric properties, and dynamic nature (rotating blades). On the other hand, hybrid methods combining Iterative Physical Optics (IPO) and SBR [20] can handle the computational load but, even though more accurate than pure SBR, still cannot account for all polarization dependent scattering mechanisms. In 2018, the polarimetric characterization of wind turbines still presents a formidable challenge for computational electromagnetics.

B. CAD models

In addition to solver technology, modeling wind turbines is difficult due to a lack of reliable knowledge regarding the CAD model. Indeed, manufacturers do not willingly divulge this information and, as a result, material distribution as well as surface curvature are only approximately known.

For instance, one common approximation is to consider purely metallic blades, which have in fact long ago been abandoned. Therefore, all transmission-related scattering mechanisms are ignored. This is an issue because all blades are in fact reinforced by a spar, which can have a very different RCS if made of glass fiber, as in previous wind turbine generations, or carbon fiber, as in the latest [18]. Another common approximation is to consider only one wind turbine model. However, to provide an optimum angle of attack all along the leading edge, newer generation blades are twisted from to bottom unlike earlier generations. Consequently, RCS can be quite different from one wind turbine to the next.

Finally, not much is known about the actual material anisotropy of composites, which has a direct impact on polarization response.

ACKNOWLEDGMENT

We acknowledge funding from the Agence De l'Environnement et de la Maîtrise de l'Energie (ADEME) in the framework of the PADIS project.

REFERENCES

[1] http://gwec.net/global-figures/graphs/

[2] https://cleantechnica.com/2018/01/06/44-wind-denmark-smashed-already-huge-wind-energy-records-2017/

[3] E. B. Arnett *et al.*, "Patterns of Bat Fatalities at Wind Energy Facilities in North America," The Journal of Wildlife Management, vol.72, pp.61-78 (2008).

[4] https://www.energy.gov/eere/wind/downloads/federal-interagency-wind-turbine-radar-interference-mitigation-strategy
https://www.anfr.fr/publications/dossiers-thematiques/eoliennes-et-radars/

[5] https://electrek.co/2017/11/02/worlds-tallest-wind-turbine-built-in-germany/

[6] https://www.aiche.org/chenected/2015/11/concrete-wind-turbine-towers-will-turbocharge-industry-growth

[7] https://www.thewindpower.net

[8] http://www.meteofrance.com/accueil

[9] https://www.arcep.fr/

[10] J. R. Probert-Jones, "The radar equation in meteorology", Quarterly Journal of the Royal Meteorological Society, vol.88, pp.485-495 (1962).

[11] D. S. Zrnić e*t al.*, "Correlation Coefficients between Horizontally and Vertically Polarized Returns from Ground Clutter", Journal of Atmospheric and Oceanic Technology, vol.23, pp.381-394 (2006).

[12] E. F. Knott *et al.*, Radar Cross Section, 2nd ed., Boston-London: Artech House, 1993, p.72.

[13] B. M. Kent *et al.*, "Dynamic Radar Cross Section and Radar Doppler Measurements of Commercial General Electric Windmill Power Turbines Part I: Predicted and Measured Radar Signatures", IEEE Antennas and Propagation Magazine, vol.50, pp.211-219 (2008);J. Pinto *et al.*, "Stealth technology for wind turbines", IET Radar, Sonar & Navigation, vol.4, pp.126-133 (2010);D. Jenn and C. Ton, "Wind Turbine Radar Cross Section", International Journal of Antennas and Propagation, vol.2012, pp.1-14 (2012).

[14] H. Ling *et al.*, "Shooting and bouncing rays: calculating the RCS of an arnitrarily shaped cavity", IEEE Transactions on Antennas and Propagation, vol.37, pp.194-205 (1989).

[15] A. Michaeli, "Equivalent Edge Currents for Arbitrary Aspects of Observation", IEEE Transactions on Antennas and Propagation, vol.32, pp.227-258 (1985).

[16] K. M. Mitzner, "Incremental Length Diffraction Coefficients", Technical Report n°AFAL-TR-73-296, Northtrop Corporation, Aircraft Division (1974).

[17] H. Azodi *et al.*, "A Fast 3-D Deterministic Ray Tracing Coverage Simulator Including Creeping Rays Based On Geometry Voxelization Technique", IEEE Transactions on Antennas and Propagation, vol.63, pp.210-220 (2015).

[18] J. J. McDonald *et al.*, "Radar-Cross-Section Reduction of Wind Turbines (Part 1)", Technical Report, n°SAND2012-0480, Sandia National Laboratories (2012).

[19] T.-Q. Fan *et al.*, "A Novel OpenGL-Based MoM/SBR Hybrid Method for Radiation Pattern Analysis of an Antenna Above an Electrically Large Complicated Platform", IEEE Transactions on Antennas and Propagation, vol.64, pp.201-209 (2016); B. Motz and T. Weiland, "Embedding the shooting and bouncing rays method in a hybrid solver framework", Applied Computational Electromagnetics Society (ACES) Symposium (2018).

[20] A. Pajot *et al.*, "Robust and GPU-accelerated IPO to improve high frequency EM scattering from large scale radar scene simulation", International Radar Conference (2014).